Experimental results of Analog-to-Information converter using Non Uniform Wavelet Bandpass Sampling for RF application

Michaël Pelissier, William Guicquero, Laurent Ouvry
Univ. Grenoble Alpes, CEA, LETI, F-38000 Grenoble

***Abstract*— Feature extraction from radio-frequency signal finds use in a growing number of applications. In cognitive radio solutions, spectral occupancy measurements, interferer energy estimation and modulation schemes recognition are some examples of such relevant features. Regarding radar applications, radio-frequency features are related to direction, time-of-arrival, or even Doppler characteristics. Recently, we introduced a novel Analog-to-Information converter architecture, referred to as Non-Uniform Wavelet Bandpass Sampling. In this paper, we present experimental results of this solution for cognitive radio application. The exploited ASIC performs compressive acquisition with power consumption as low as 225 pJ/meas for a RF signal in the GHz range. An experimental phase transition graph is reported with a comparison with its theoretical counterpart.**

***Keywords* — Analog-to-information conversion, cognitive radio, radar, compressive sensing, wavelets, spectrum sensing.**

I. INTRODUCTION

Compressive sensing (CS)-based A2I converters are a promising solution for wideband radiofrequency (RF) direct feature extraction either for cognitive radio or radar. Under proper signal structure assumptions (basically consisting in sparsity in some basis), CS enables the acquisition of larger bandwidths with relaxed sampling-rate requirements, thus enabling inexpensive, faster, and potentially more energy-efficient solutions than traditional Nyquist Analog-to-Digital Converters (ADCs) [1]. Recently, we have proposed a novel Analog-to-Information (A2I) converter referred to as Non-Uniform Wavelet Bandpass Sampling (NUWBS) [2]. This architecture combines wavelet pre-processing with non-uniform sampling, which mitigates the key issues of existing A2I solutions, such as noise, aliasing, and relax timing constraints. Wavelet processing is widely used for natural image compression, time-frequency analysis and demonstrate its efficiency for MRI [3]. However, time-scale wavelet analysis is far less explored in RF applications. In [4], the authors first introduce a method for spectrum estimation and detection with a wavelet based edge detector combining continuous wavelet transform on spectral density, multi-resolution analysis and compressive sensing. In [5] the authors investigate the wavelet packet decomposition for new spectrum sensing. At last, the authors of [6] propose a multichannel scheme based on Gabor frames that takes advantage of signals temporal sparsity and enables sampling multi-pulses signals at sub-Nyquist rates extending the concept of Modulated Wideband Converter for impulse RADAR application. Wavelet processing and our solution, NUWBS, could be advantageously used for cognitive radio solution. For instance, NUWBS architecture could be seen as an add-on to a main high-end RF front end. This add-on senses specific features in RF spectrum and provides relevant information to the main receiver for re-configurability purposes. With respect to radar applications, CS has recently opened a new path to sensor design with relaxed constraints compared to traditional Nyquist-rate sensing [7]. In particular in [8], for Range-Doppler estimation, the technique takes advantage of sparsity priors on the Ambiguity Functions surfaces. This particularly suits the NUWBS strategy which offers flexible control on time-frequency windows for adaptive CS.

In this paper, we present experimental results based on a hardware platform demonstrating NUWBS performances in terms of transition graph for RF spectral sensing. The paper is organized as follows. Section II reminds the basics of NUWBS architecture and the related analytical framework. Section III provides insight on the hardware platform and the ASIC front-end used to perform compressive acquisition. Section IV describes the measurement results including experimental phase transition graph. We conclude and suggest future work directions in section V.

II. COMPRESSIVE ACQUISITION WITH NON UNIFORM WAVELET BANDPASS SAMPLING (NUWBS)

A. Compressive Sensing framework and notation

Let $\mathbf{x} \in \mathbb{R}^N$ be a discrete time, N dimensional real signal that we wish to acquire using a CS strategy. We assume that the signal $\mathbf{x}$ has a so-called K-sparse representation $\mathbf{s} \in \mathbb{C}^N$ (i.e. the vector $\mathbf{s}$ has K dominant non-zero entries, $\|\boldsymbol{s}\|_0 = K$) in a known (unitary) transform basis $\boldsymbol{\Psi} \in \mathbb{C}^{N \times N}$ with $\mathbf{x} = \boldsymbol{\Psi}\mathbf{s}$ and $\boldsymbol{\Psi}^H\boldsymbol{\Psi} = \mathbf{I}_N$. In spectrum sensing applications we first target, one typically assumes sparsity in the DFT basis, i.e., $\boldsymbol{\Psi} = \mathbf{F}^H$ ($\mathbf{F}^H$ is the N-dimensional inverse DFT matrix). CS performs M compressive measurements in the form of a set of inner products denoted as $\boldsymbol{y}_i = \langle \boldsymbol{\phi}_i, \boldsymbol{s} \rangle$ for i =1..M where $\boldsymbol{\Phi}_i$ are the measurement vectors of the sensing matrix $\boldsymbol{\Phi}$. In the absence of noise, the CS measurement process can be written in compact matrix-vector form as follows:

$$\mathbf{y} = \boldsymbol{\Phi}\mathbf{x} = \boldsymbol{\Phi}\boldsymbol{\Psi}\,\mathbf{s} = \boldsymbol{\Theta}\,\mathbf{s} \quad \text{with } \boldsymbol{\Theta} = \boldsymbol{\Phi}\boldsymbol{\Psi}. \tag{1}$$

The M×N matrix $\boldsymbol{\Theta}=\boldsymbol{\Phi}\boldsymbol{\Psi}$ models the joint effect of CS and the sparsifying transform. The main goal of CS is to acquire far fewer measurements than the ambient dimension N, i.e., we are interested in the case where M<< N. This implies that the matrix $\boldsymbol{\Theta}$ maps K-sparse signals of dimension N to a small number of measurements M.

B. *Principle of the NUWBS architecture*

The principle of NUWBS is illustrated in Fig. 1. In comparison with classical Non-Uniform Sampling (NUS), NUWBS first transforms the incoming analog time signal $x(t)$ into a wavelet frame $\mathcal{W}x(t)$ before performing NUS on the resulting coefficient [2]. The wavelet transform is directly performed in the time domain. The process could be split into three steps i) The multiplication of the input signal $x(t)$ with wavelets comb $p_c(t)$, ii) The integration and dump over a period T_i and iii) The non-uniform sampling of the resulting wavelet coefficients at a sub-Nyquist rate f_s. The wavelet comb lays on a regular sampling grid, sub-sampled in time with respect to the Nyquist rate achieving band-pass sampling. The compression is due to sub-sampling ratio $\gamma = f_{Nyq}/f_s$ combined with a random selection of wavelet coefficient among the available ones. The overall sensing strategy thus benefits from a twofold dimension reduction with respect to the original Nyquist band.

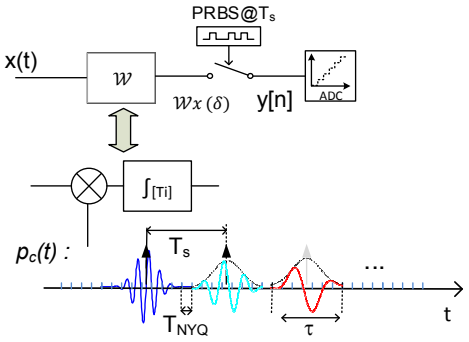

Fig. 1 Overview of the NUWBS architecture.

C. *Analytical framework of NUWBS architecture*

In discrete time, the sensing matrix $\mathbf{\Phi}$ for NUWBS can be described by taking a set Ω of rows of a wavelet frame denoted $\mathbf{W}^{\mathrm{H}} \in \mathbb{C}^{|\Omega| \times N}$. $|\Omega|$ defines the number of available wavelets in the frame. $\boldsymbol{R_\Omega}$ defines the row selector operator that picks up uniformly at random M wavelets among the $|\Omega|$ available so that $M \leq |\Omega|$. Hence, the sensing matrix of NUWBS is $\boldsymbol{\Phi_{NUWBS}} = \boldsymbol{R_\Omega W^H}$. We can describe the NUWBS process as:

$$\boldsymbol{y} = \boldsymbol{R_\Omega W^H x} = \boldsymbol{\Theta_{NUWBS} s}. \quad (2)$$

with the sensing matrix $\boldsymbol{\Theta_{NUWBS}} = \boldsymbol{R_\Omega W^H F^H}$. As a result NUWS subsamples the matrix $\mathbf{A}=(\mathbf{FW})^{\mathrm{H}}$, which is the Hermitian (or self-adjoint) of the Fourier transform of the entire wavelet frame. Depending on its time shift and scale, each wavelet captures a different portion of the spectrum with respect to a given phase and bandwidth defined around a center frequency. In this paper, we consider a set of Gabor atoms – even if not, mathematically speaking, a wavelet basis –, but however, is very similar to an overcomplete dictionary [9]. In practice, each atom is defined as a Gaussian window modulated by a complex exponential. Our Gabor atoms therefore consist of functions parametrized by their temporal width τ, center frequencies f_v^c and time shifts δ_k. Time and frequency representations of l2-normalized Gabor atoms [2] are defined as with k=1,…, $|\Omega|$:

$$\psi_{f_v^c,\delta_k}(t) = \frac{2^{\frac{1}{4}}}{\sqrt{\tau}\,\pi^{\frac{1}{4}}} e^{j2\pi f_v^c (t-\delta_k)} e^{-\left(\frac{t-\delta_k}{\tau}\right)^2}, \quad (3)$$

$$\Psi_{f_v^c,\delta_k}(f) = (\tau\sqrt{2\pi})^{\frac{1}{2}} e^{-j2\pi\delta_k f} e^{-(\pi\tau\,(f-f_v^c))^2}. \quad (4)$$

D. *Benefits of RF wavelet processing and the NUWBS architecture*

From a hardware perspective, NUWBS has the following advantages. Unlike the NUS approach, the wavelet transform $\mathcal{W}$ reduces the bandwidth of the input signal $x(t)$, thus relaxing the bandwidth of the S&H circuit and the ADC. Also, many alternative CS-based A2Is require Nyquist rate circuits to generate random sequences [10] or clocks [11] unlike NUWBS solution. In addition, NUWBS enables full control over a number of parameters such as the sample time instants, the wavelet bandwidth and the center frequency. Thanks to this sensing tunability, the measurement strategy can be adjusted depending on the signal priors and the target application thus allowing the development of an adaptive CS framework. Also, traditional bandpass sampling or other CS methods for multi-band signals highly suffer from noise and interferers aliasing [12]. On the contrary, wavelet selection of NUWBS enables to arrange the time-frequency tiling in a manner that minimizes the disturbances and renders the solution which is resilient to out-of-band noise and interferers. The wavelet center frequency focuses on the sub-bands of interest while its envelope acts as an equivalent filter. At last, NUWBS consists in a convenient structure that performs a sensing scheme reducing acquisition matrix storage needs and recovery algorithm complexity, unlike its fully randomized counterpart.

III. Hardware Platform Description of Non Uniform Wavelet Bandpass Sampling Solution (NUWBS)

A. *ASIC description for Wavelet Bandpass sampling solution*

We now target to implement NUWBS solution with a practical hardware setup. From the general framework described in previous sections, we derivate the practical case study to the case where wavelet have a fixed central frequency f_v^c and duration τ along the different atoms. Only the wavelet time shift δ_k is made variable in the closed form equation (3) and could be associated somehow to random filtering. Originally designed for coherent impulse Ultra Wide Band reception application, our ASIC (Application-Specific Integrated Circuit) depicted in [13] is used. This ASIC embeds wavelet stream generation centered at 4GHz (f_v^c) with a periodic rate $f_s = 1/T_s$. Then, mixing, integration over a time duration T_i and dump features are performed (Fig. 1). The I/Q output signal accounts for to the complex wavelet coefficients. With this ASIC, wavelet combs generation, wavelet projection including signal amplification and correlation could be performed with an energy as low as 225pJ/projection [13].

B. *Hardware platform description*

Fig. 2 shows the NUWBS hardware validation platform. An arbitrary waveform generator AWG7122C, feeds in the platform a K-frequency sparse real signal in the vicinity of the wavelet central frequency f_v^c = 4GHz within a bandwidth BW_{RF}

of 125MHz defining the frequency a sub-space Σ. The AWG generates unitary-amplitude K tones on a frequency grid with a frequency resolution $\Delta f = 1/T_{acq}$ with T_{acq} defining the overall acquisition time T_{acq}. The signal corresponds to an N-dimensional input vector **x** at a Nyquist rate f_{NYQ} and is directly loaded from Mathworks® environment. The wavelet rate f_s is adjusted by an external clock signal leading to an equivalent wavelet rate f_s =125MHz. It leads to a maximum of |Σ|=64 wavelet coefficients per acquisition time T_{acq} (|Σ|=T_{acq}/T_s). At the output, the analog complex (I/Q) wavelet coefficients corresponding to vector **y** is digitalized by a sampling scope. To get rid of any parasitic noise effects, the scope averages each coefficient over 16 iterations. Measurement data are then transferred to the Mathworks® to perform a CS recovery algorithm. Table I summarizes the parameter settings of the hardware platform.

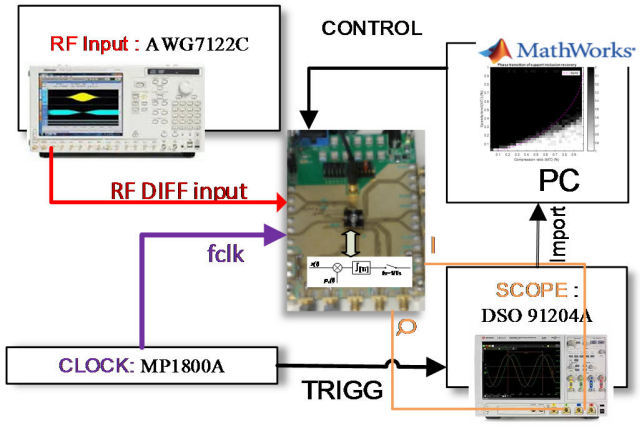

Fig. 2 : NUWBS hardware validation platform

TABLE I. NUWBS HARDWARE PLATFORM SETTINGS

Parameters description	*Name*	*Typical value*	*Comment*
Nyquist rate	f_{Nyq}	32 GHz	
Resolution frequency	Δf	1.9531MHz	= f_{NYQ} /N
Acquisition time	T_{acq}	512 ns	=1/Δf
Wavelet central frequency	f_v^c	4.0 GHz	
Wavelet duration	τ	2.75 ns	
Wavelet repetition Frequency = Sampling frequency	f_s	125 MHz	= 1/Ts
Sensing bandwidth	BW_{RF}	125 MHz	
Subsampling ratio	γ	256	= f_{NYQ}/f_s = N/|Σ|
Number of wavelet Coefficients per acquisition Time	|Σ|	64	= T_{acq}/Ts = $BW_{RF}/\Delta f$ = N/ γ

IV. EXPERIMENTAL RESULTS OF NUWBS FOR RF SIGNAL ACTIVITY DETECTION

In this application, we target RF activity detection, which is equivalent to frequency support recovery. From $\boldsymbol{y}$ acquired by the platform, spectral support of **s** is recovered using orthogonal matching pursuit algorithm (OMP). This sparse approximation algorithm requires the knowledge of a properly characterized measurement matrix $\Theta_{\mathbf{NUWBS}}$ and can also takes advantage of knowing the sparsity degree K. Section A describes the learning phase of the acquisition matrix $\Theta_{\mathbf{NUWBS}}$ needed by the recovery algorithm. Section B gives the typical RF scenario considered for activity detection. Section C provides a better insight of measured CS vector $\boldsymbol{y}$ and compares measurements with a theoretical approach. At last, Section D shows and discusses the full transition graph performance of the proposed solution.

A. Learning of the experimental acquisition matrix A

The OMP requires the acquisition matrix used for the compressive measurement $\Theta_{\mathbf{NUWBS}} = \boldsymbol{R_\Omega}(\boldsymbol{FW})^{\boldsymbol{H}}$ defined in (2). The row selector $\boldsymbol{R_\Omega}$, selecting M measurements out of |Σ| is straightforwardly obtained since it corresponds to the wavelet index k selected from 1..|Σ|. However, in the matrix $\Theta_{\mathbf{NUWBS}}$ expression, the matrix $\boldsymbol{A} = (\boldsymbol{FW})^{\boldsymbol{H}}$ needs to be accurately characterized in order to employ the OMP algorithm. This greedy algorithm is a basic one, not robust to noise issues but well suited to demonstrate the intrinsic performances of the hardware without any algorithm trick. The matrix $\boldsymbol{A}$ only depends on the ASIC characteristics and can be acquired once forever. The objective of this section is to measure this experimental acquisition matrix provided by the hardware platform. To do so, we sweep the input frequency $f_i = \nu_i \Delta f$ over a frequency range from 2.5GHz to 5 GHz. The frequency of the output signal f_{out} fold into [$-f_s/2$; $f_s/2$] and in the case of a single tone input, f_{out} is linked to the input frequency f_i by the following equation:

$$f_{out} = f_i - f_s \left\lfloor \frac{f_i}{f_s} \right\rceil \text{ with } \lfloor\ \rceil \text{ the round operator.} \qquad (5)$$

Discrete Fourier Transform (DFT) is computed to extract the magnitude of the signal at f_{out}. It leads to the module of any rows of **A** noted $|\boldsymbol{A}_{k,:}|$ for k=1..|Σ|. The matrix module accounts for the filtering property of the NUWBS solution [2] acting like a transfer function. On Fig. 3 the measured −10dB bandwidth of the transfer function module is 300 MHz. Fig. 3 shows also experimental argument of the acquisition matrix **A** which depends on row index k in accordance with theoretical expression extracted from (4) :

$$Arg(\boldsymbol{A}_{k,:}) = -2\pi k T_s \upsilon \Delta f. \qquad (6)$$

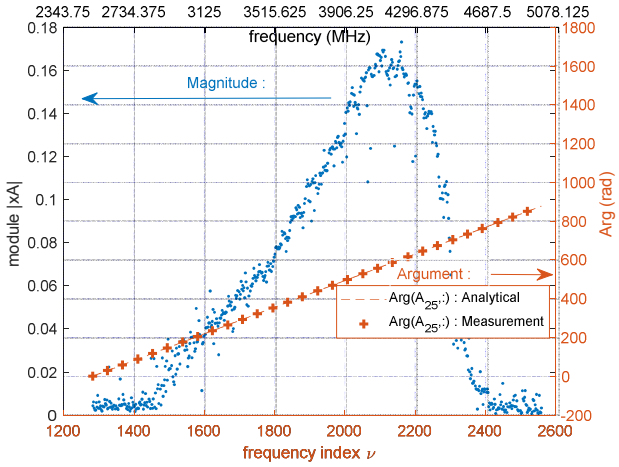

Fig. 3 : Magnitude and Argument of the experimental matrix **A** (f>0)

B. *Compressive sensing acquisition scheme*

With regard to the RF signal activity detection scenario, we consider a single active sub-band of interest BW_{RF} among the entire Nyquist band denoted f_{Nyq}. The total number of potentially active frequency bins within BW_{RF} is denoted $|\Sigma|$ = 64. The spectral sensing functionality of the system consists in finding what the active bins within the overall available $|\Sigma|$ are.

The real signal is assumed to be $K \leq |\Sigma|$ sparse. The NUWBS measurements are selected according to the illustration provided on Fig. 4. We set in the ASIC a constant wavelet central frequency f_v^c = 4GHz, duration τ and repetition frequency fs to 125 MHz. It leads to a sub-sampling ratio $\gamma = f_{Nyq}/f_s$ of 256. The sub-sampling ratio is inherent to the bandpass sampling property of NUWBS solution. In addition, NUS of the wavelet coefficient allows a selection of M coefficients out of the $|\Sigma|$ available, thus performing the compressive operation.

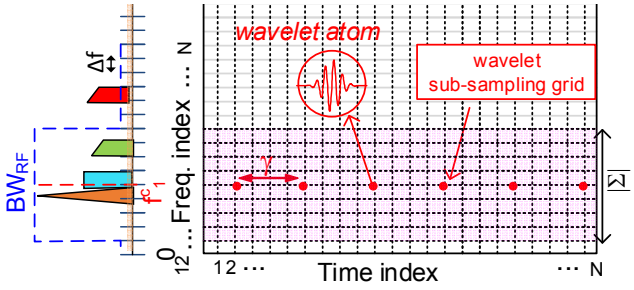

Fig. 4 : Illustration of sampling scheme of NUWBS validation platform

Fig. 5 provides a comprehensive overview of the sensing scheme used in the validation hardware platform. In this scenario, a sparse signal occupies K = 8 bins (green) among $|\Sigma|$ = 64 bins available (dark blue) from ν = 2144..2176 with unitary-amplitude. In addition, it can be noticed that the magnitude of the experimental acquisition matrix **A** for $f > 0$ (soft blue) and the analytical behavioral model of the wavelet envelop (magenta) are overlaid.

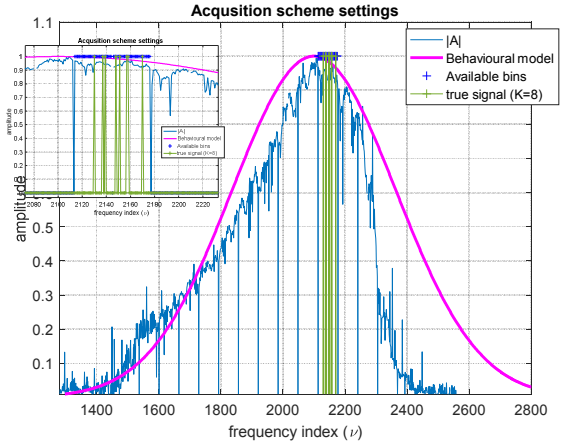

Fig. 5 : Illustration of compressive sensing acquisition scheme [K=8 activated bins (green) within BW_{RF} ={2114…2176}Δf] - Comparison with the magnitude of acquisition matrix |**A**| (soft blue) and analytical behavioral model of wavelet envelop (magenta)

C. *Analysis of typical compressive sensing wavelet coefficient*

For the sake of illustration, Fig. 6 exhibits i) the compressive sensing measurement vector **y**, ii) the product $\boldsymbol{A} \times \boldsymbol{s}$ between the experimental acquisition matrix (from previous section) and the generated input signal spectrum **s**, and iii) directly the sum of the relevant column index the experimental acquisition matrix $y_k = \sum_{\nu \epsilon \Lambda} A_{k,\nu}$ where Λ represents the input signal support. The illustration corresponds to the acquisition scenario described in the previous section (K = 8). Each value of the measurement vector y_k for k = 1…$|\Sigma|$ accounts for a wavelet coefficient corresponding to the projection of input signal $x(t)$ on the wavelet atom $\psi_{f_v^c,\delta_k}(t)$. The experimental acquisition matrix $\boldsymbol{A}$ includes delay re-synchronization between wavelet comb and input signal so that we have a proper matching between measurement and analytical computation. This has been validated along the case where measurement vector **y** is full (i.e. M = Σ = 64) and with compression rate of 0.5 (M = 32) as illustrated on Fig. 6.

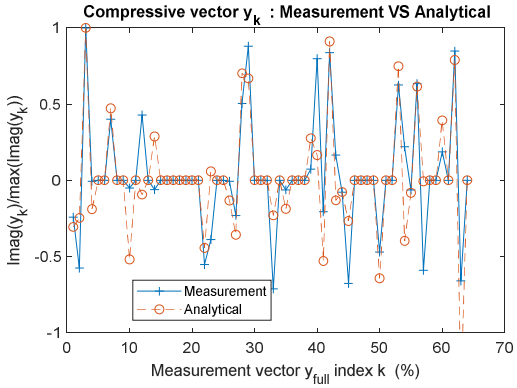

Fig. 6 : Normalized Imaginary values of CS vector y[k] and comparison with analytical results (**A×s)** [K=8; M=32; |Σ|=64]

D. *Transition graph measurement*

Once compressive measurements are performed, the spectral support of **s** is recovered based on a standard OMP algorithm fed by the sparsity degree K and the experimental acquisition matrix $\Theta_{\mathbf{NUWBS}}$. Moreover, the reconstruction is restricted to the sub-bands of interest, assuming that the knowledge of the sub-band support Σ is an additional prior. The usage of the OMP is therefore limited to find the K active coefficients within these sub-bands. As result, we measure an experimental phase transition graph that characterizes the probability of correct support recovery from NUWBS measurements [14]. To carry out this exhaustive characterization, we generate measurement-sparsity pairs (M, K) and perform support set recovery for 100 Monte–Carlo trials and report the average of the error probability Pe. A success is declared if and only if all the bins locations are correctly detected by the algorithm. On Fig. 7 the phase transition graph is plotted a grayscale image where the pixel intensity represents the probability of error. Magenta plain line is the reference baseline and minimum bound, corresponding to the theoretical phase transition plan of l1-norm based sparse signal recovery for a Gaussian measurement ensemble [14]. We can observe a suitable fitting between theoretical equation and measurement results especially at low sparsity degree where OMP algorithm is known to be the most efficient. To provide better insight on performances, Fig. 8 shows specific sparsity level corresponding to cut plan of the

full transition graph reported on Fig. 7.

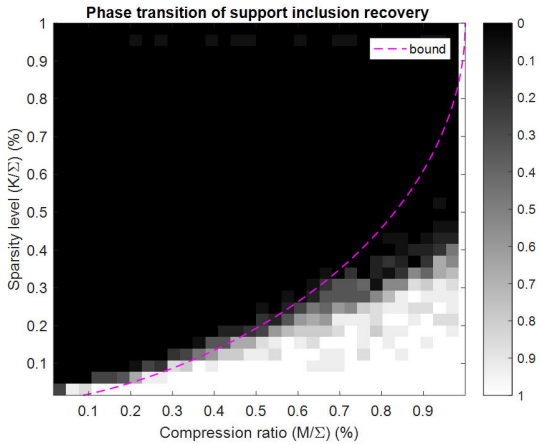

Fig. 7 : Experimental Transition graph cuts of NUWBS solution

The error probability is plotted as a function of compression ratio M/|Σ| for several relative sparsity degree K (K=1, 2, 4, 6, 8). Dash line corresponds to the expected theoretical performances while plain line with a cross marker is the compressive measurement vector **y** measured in practice. These results demonstrate the functionality of the non-uniform wavelet bandpass sampling NUWBS to perform support recovery of RF signal.

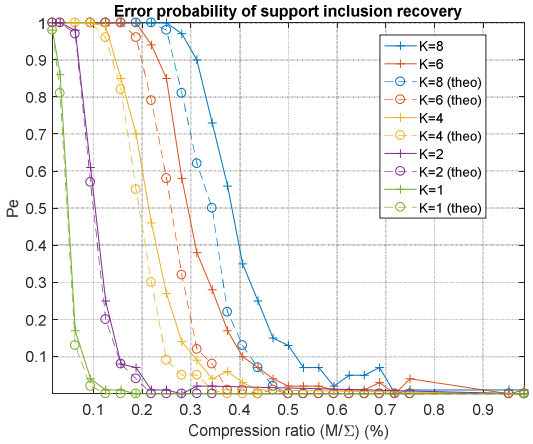

Fig. 8 : Experimental Transition graph cuts of NUWBS solution

V. Conclusion and Future Work

The NUWBS architecture is a promising solution for RF applications. This solution could be applied for RF features extraction either in cognitive radio context or radar application. In this paper, we exploit NUWBS for spectrum sensing capability i.e., support detection of frequency sparse signal. The hardware platform uses a power efficient ASIC implementing NUWBS RF front end. The solution does not require either fast Nyquist rate components or converter with high analog bandwidth. This ASIC performs compressive acquisition with power consumption as low as 225 pJ/meas for an RF signal in the GHz range. Acquisition matrix learning phase is presented so as to characterize NUWBS RF front end. Experimental transition graph is provided and shows a decent matching between theoretical and practical approaches especially when the sparsity degree K is low. Future work directions are many-fold. Parametric analysis on circuit parameters could be performed to evaluate sensitivity of CS approach to RF impairments including noise performances analysis. Also, alternative recovery algorithm to OMP could be benchmarked on the same platform to estimate the impact of the different noise sources. Furthermore, CS-based RF feature extraction could be pursued for direct signal classification either for cognitive radio or radar application.

Acknowledgment

The NUWBS solution was developed in partnership with Cornell University, C. Studer's group, with the support of FR Enhanced Eurotalents fellowships program & Carnot Institute, and under US NSF grants CCF-1535897, ECCS-1408006, and CAREER CCF-1652065. The platform utilized ASIC developed within the RUBY project supported by the FR National Agency for Research (ANR).

References

[1] S. K. Sharma, E. Lagunas, S. Chatzinotas, and B. Ottersten, "Application of Compressive Sensing in Cognitive Radio Communications: A Survey," *IEEE Communications Surveys & Tutorials,* vol. 18, pp. 1838-1860, 03 Feb 2016 2016.

[2] M. Pelissier and C. Studer, "Non-Uniform Wavelet Sampling for RF Analog-to-Information Conversion," *IEEE Transactions on Circuits and Systems I: Regular Papers,* vol. 65, pp. 471-484, 2018.

[3] T. Strohmer, "Measure What Should be Measured: Progress and Challenges in Compressive Sensing," *Signal Processing Letters, IEEE,* vol. 19, pp. 887-893, 2012.

[4] T. Zhi and G. B. Giannakis, "Compressed Sensing for Wideband Cognitive Radios," in *Acoustics, Speech and Signal Processing, 2007. ICASSP 2007. IEEE International Conference on*, 2007, pp. IV-1357-IV-1360.

[5] M. K. Lakshmanan and H. Nikookar, "A Review of Wavelets for Digital Wireless Communication," *Wireless Personal Communications,* vol. 37, pp. 387-420, 2006.

[6] E. Matusiak and Y. C. Eldar, "Sub-Nyquist sampling of short pulses," in *2011 IEEE International Conference on Acoustics, Speech and Signal Processing (ICASSP)*, 2011, pp. 3944-3947.

[7] J. Ender, "A brief review of compressive sensing applied to radar," in *2013 14th International Radar Symposium (IRS)*, 2013, pp. 3-16.

[8] I. Kyriakides, "Adaptive Compressive Sensing and Processing of Delay-Doppler Radar Waveforms," *IEEE Transactions on Signal Processing,* vol. 60, pp. 730-739, 2012.

[9] O. Christensen, "Pairs of dual Gabor frame generators with compact support and desired frequency localization," *Applied and Computational Harmonic Analysis,* vol. 20, pp. 403-410, 2006.

[10] M. Mishali and Y. C. Eldar, "From Theory to Practice: Sub-Nyquist Sampling of Sparse Wideband Analog Signals," *Selected Topics in Signal Processing, IEEE Journal of,* vol. 4, pp. 375-391, 2010.

[11] D. E. Bellasi, L. Bettini, C. Benkeser, T. Burger, H. Qiuting, and C. Studer, "VLSI Design of a Monolithic Compressive-Sensing Wideband Analog-to-Information Converter," *Emerging and Selected Topics in Circuits and Systems, IEEE Journal on,* vol. 3, pp. 552-565, 2013.

[12] E. Arias-Castro and Y. C. Eldar, "Noise Folding in Compressed Sensing," *IEEE Signal Processing Letters,* vol. 18, pp. 478-481, 2011.

[13] L. Ouvry, G. Masson, F. Hameau, B. G. Gaillard, and B. Caillat, "A CMOS Duty-Cycled Coherent RF Front-End IC for IR-UWB Systems," in *2015 IEEE International Conference on Ubiquitous Wireless Broadband (ICUWB)*, 2015, pp. 1-5.

[14] D. L. Donoho, A. Maleki, and A. Montanari, "Message-passing algorithms for compressed sensing," *Proceedings of the National Academy of Sciences,* vol. 106, pp. 18914-18919, 2009.